Fiber-Optic Enzyme Biosensor for Direct Determination of Organophosphate Nerve Agents

Ashok Mulchandani,* Shengtian Pan, and Wilfred Chen

Department of Chemical and Environmental Engineering, University of California, Riverside, California 92521

A fiber-optic enzyme biosensor for the direct measurement of organophosphate nerve agents was developed. The basic element of this biosensor is organophosphorus hydrolase immobilized on a nylon membrane and attached to the common end of a bifurcated optical fiber bundle. The enzyme catalyzes the hydrolysis of organophosphate compounds to form stoichiometric amounts of chromophoric products that absorb light at specific wavelengths. The back-scattered radiation of the specific incident radiation was measured using a photomultiplier detector and correlated to the organophosphate concentration. The effects of buffer pH, temperature, and the units of enzyme immobilized on the steady-state and kinetic response of the biosensor were investigated to optimize the operating conditions for the fiber-optic enzyme biosensor. These conditions were then used to measure parathion, paraoxon, and coumaphos selectively without interference from carbamates and triazines. Concentrations as low as 2 μM can be measured in less than 2 min using the kinetic response. When stored in buffer at 4 °C the biosensor shows long-term stability.

Introduction

The acute toxicity of organophosphorus neurotoxins (nerve agents) and their widespread use in modern agricultural practices have increased public concerns, which have stimulated the development of technologies to effectively treat effluents generated at both the producer and consumer levels (*1*−*6*). Additionally, the recently ratified Chemical Weapons Treaty requires the United States to destroy all of its chemical weapons arsenal, including the organophosphorus-based nerve gases, within 10 years (*7, 8*). The successful use of any technology for detoxification of the organophosphate nerotoxins will require analytical tools for monitoring concentrations of these neurotoxins.

Biosensors based on acetylcholinesterase (AChE) inhibition have been investigated over the past decade (*9*). Although sensitive and useful as single-use devices for environmental monitoring, AChE-based biosensors are however not suitable for on-line monitoring of detoxification processes. The analyses with AChE-based biosensors require a long and tedious protocol involving long incubation with inhibitors prior to analysis for good sensitivity and treatment with pyridine-2-aldoxime after analysis for partial regeneration/recovery of the enzyme activity which is inhibited irreversibly by OP (*10*−*12*). Additionally, since AChE is also inhibited by other neurotoxins such as carbamate pesticides and many other compounds, these biosensors are not selective and therefore not suitable for quantifying either an individual or a class of pesticides which may be required for monitoring detoxification process.

Organophosphorus hydrolase (OPH) hydrolyzes a range of organophosphate esters, including pesticides such as parathion, coumaphos, and acephate and chemical warfare agents such as soman, sarin, VX, and tabun (*13*−*16*). The catalytic hydrolysis of these compounds releases protons that can be measured and correlated to the OP concentration. This was the basis of the reported potentiometric enzyme and microbial electrodes (*9, 17*−*19*). The hydrolysis of several of the organophosphates also produce chromophoric products, which absorb light at specific wavelengths (*20*), that can be measured and correlated to the OP concentration. This forms the basis of the new fiber-optic enzyme biosensor (FOEB) reported in this paper.

Materials and Methods

Reagents and Materials. Organophosphorus hydrolase was produced and purified according to the methods described by Mulchandani et al. (*9*). HEPES, cobalt chloride, and glutaraldehyde were purchased from Fisher Scientific (Tustin, CA). Bovine serum albumin was obtained from Sigma Chemical Co. (St. Louis, MO). Paraoxon, parathion, diazinon, simazine, sutan, atrazine, sevin, and pentachlorophenol were acquired from Supelco Inc. (Bellefonte, PA). Biodyne nylon membrane (0.45 μm pore size) was a gift from Pall Biosupport Division (New York). All of the solutions were made in distilled deionized water.

Experimental Setup. ***Apparatus.*** The fiber-optic setup used in the study was made by assembling the components acquired from Photon Technology International, Inc. (Monmouth, NJ). The setup shown in Figure 1 consisted of a 75-W xenon arc lamp light source (Model 02-5002X), housed in PowerArc lamp housing (**b**), powered by a constant-voltage dc lamp power supply (Model LPS-220) with an igniter (Model LPS-221) (**a**), a monochromator (**c**) (Model 101) attached to one arm of the bifurcated fiber-optic bundle, set at a desired cutoff wavelength (400 nm for *p*-nitrophenol, hydrolysis product

* Corresponding author. Mailing address: College of Engineering, Bourns Hall, University of California, Riverside, CA 92521. Telephone: (909) 787-6419. Fax: (909) 787-3188. E-mail: adani@engr.ucr.edu.

10.1021/bp980111q CCC: $18.00
Published on Web 01/12/1999

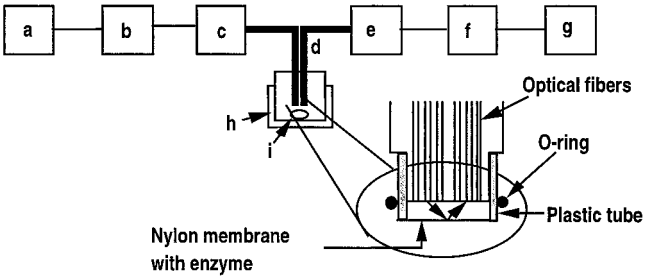

Figure 1. Schematic drawing of the FOEB and the sensor tip: (a) power supply; (b) xenon-arc lamp; (c) monochromator; (d) bifurcated optical fiber bundle; (e) monochromator; (f) photomultiplier detection system; (g) chart recorder/computer; (h) thermostated vessel; (i) magnetic stirring bar.

of paraoxon and parathion, and 348 nm for chlorferon, hydrolysis product of coumaphos), a 0.5-m bifurcated quartz fiber-optic bundle (**d**), a second monochromator (**e**), set at the same wavelength as the first one, attached to other arm of the bifurcated fiber bundle, a photomultiplier detection system (**f**) (Model 814), and a strip chart recorder (**g**) (Model BD112, Kipp and Zonen, Holland). The setup was isolated from the ambient light by thick black curtains (light modulation can be used as an alternative to curtains).

Sensor Tip. The details of the sensor tip are shown in Figure 1. It consisted of the optical fiber bundle common end (7 mm diameter) encased by an 11 mm o.d. × 12.5 mm long cylinder on which a tightly fitting plastic tube (11 mm i.d. × 1 mm thick × 13.3 mm long) with two open ends was mounted. Nylon membrane with immobilized OPH (please see below) was attached to the end of this plastic tube by an O-ring. This arrangement provided an approximately 0.8 mm gap between the optical fiber flush end and the immobilized enzyme nylon membrane, the path length for the back-scattered light.

Enzyme Immobilization. Various dilutions (20 μL) of the purified stock enzyme (activity of 33 units/μL; 1 unit = 1 μmol of *p*-nitrophenol formed per minute from hydrolysis of 0.7 mM paraoxon in pH 8.5, 50 mM HEPES + 50 μM $CoCl_2$ buffer at 25 °C) solution, 2 μL of 10% bovine serum albumin, and 5 μL of 2.5% glutaraldehyde were placed in a 1-mL Eppendorf tube and vortexed. A 20-μL sample of the mixture was then layered on 0.45 μm pore size Biodyne nylon membrane (10 μL on each side) that was held tightly to the one open end of the plastic tube extension (described above) by an O-ring. The protein layer was allowed to dry in air for 30 min and washed thoroughly with buffer (50 mM HEPES + 50 μM $CoCl_2$, pH 8.5) to remove excess glutaraldehyde and stored at 4 °C in the same buffer.

Measurements. Buffer (50 μL) was placed on the membrane before slipping it over the fiber bundle end. The sensor tip was then immersed in 5 mL of the appropriate buffer, controlled at the desired temperature, in a 10-mL working volume jacketed glass cell (**i**) equipped with a magnetic stirring bar (**h**). The temperature of the liquid in the cell was controlled by circulating water in the cell jacket using a circulating water bath (Model 1160, VWR Scientific, San Francisco, CA). At the start, the dark (background) current was recorded by closing the entrance slit of the collection monochromator. Subsequently, the entrance slit of this monochromator was opened and the incident/initial intensity (I_0) was recorded. OP nerve agent (5−10 μL), dissolved in pure methanol, was then added to the cell, and the trace of the change in light intensity as a function of time was recorded. The recorded data were used to determine the

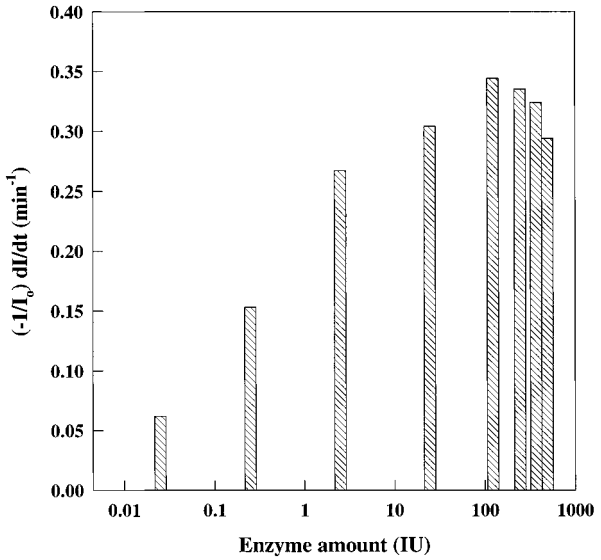

Figure 2. Effect of enzyme loading on the response of the FOEB to 0.42 mM paraoxon in pH 8.5, 50 mM HEPES + 0.05 mM $CoCl_2$ at 30 °C.

steady-state and kinetic response of the FOEB. The steady-state absorbance was calculated from (eq 1),

$$A_s = \log I_0/I_s \quad (1)$$

where I_s is the steady-state intensity. For the kinetic response measurement, the initial rate of change of absorbance was determined from (eq 2), where dI/dt is the initial rate of intensity change (the slope of the tangent to the response curve at $t = 0$).

$$dA/dt = -(1/I_0)dI/dt \quad (2)$$

Results and Discussion

Effect of Various Parameters on the Response of FOEB. The heterogeneous nature of the biosensor configuration results in either the enzyme kinetics or the mass transport to be the rate-limiting step in sensor response. The kinetic response of the sensor is independent of the amount (units) of enzyme when saturating amounts of enzyme are immobilized on the sensor tip. Below this saturation point, however, the kinetic response is strongly affected by the immobilized enzyme amount. As can be seen in Figure 2, initially the magnitude of the OPH-modified FOEB (OPH was immobilized on 0.45-μm Biodyne nylon membrane) response increased steeply with increasing enzyme units and subsequently reached a plateau for enzyme loading above 123 units. Beyond this saturating amount, the response showed a small decrease due to the increased enzyme layer thickness, resulting from increased protein amount, thus slowing the mass transport rate. The region where mass transfer is controlling is preferred for enzyme-based sensors since in this region the response of the biosensor becomes relatively insensitive to alterations in enzyme activity and thus prolongs the biosensor operational and storage lifetimes (*21*). The OPH loading of 123 units was therefore selected for all subsequent experiments.

The operating temperature of the FOEB affected the response of the OPH-modified FOEB. The response initially increased with temperature up to 55 °C and then decreased with any further temperature increase (data not shown). The initial increase in the rate is attributed to the increase of both the enzyme reaction and mass

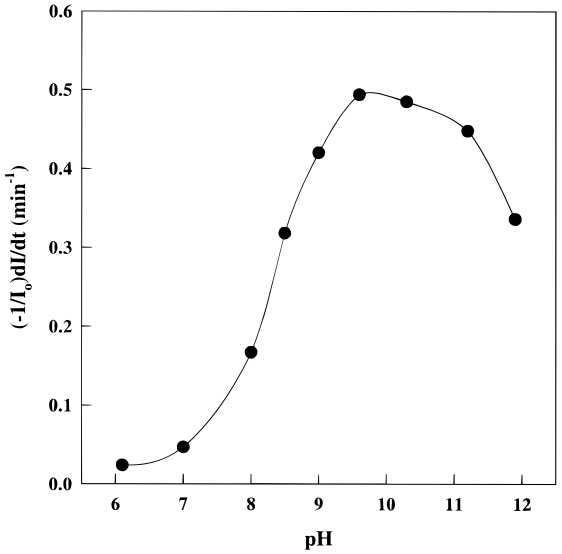

Figure 3. Effect of pH on the response of the FOEB to 0.42 mM paraoxon in 50 mM HEPES + 0.05 mM $CoCl_2$ buffer at 30 °C; 123 IU of OPH immobilized on 0.45-μm nylon membrane.

transport rates. The decrease in the rate at higher temperatures is due to enzyme denaturation. This temperature profile is in accordance with that reported for the free enzyme (*22*).

The FOEB response was also a function of pH (Figure 3). The observed pH profile was similar to that of the free and immobilized enzyme (*9*). This, in conjunction with the fact that there was no change in the absorbance when there was no enzyme immobilized at the fiber tip, confirmed that the observed pH dependence of the sensor response was due to the pH dependence of the OPH activity. pH 9 was selected for subsequent investigations.

Analytical Characteristics of FOEB. ***Calibrations for Organophosphates.*** As displayed in the representative photomultiplier tube voltage output-time readings obtained with the FOEB (Figure 4), the initial rate and the total change of voltage, i.e., intensity, are functions of OP concentration. Table 1 summarizes the important analytical characteristics of OPH-based FOEB for the different analytes investigated. (Although 55 °C was determined to be the optimum temperature for the FOEB operation, calibration plots and stability evaluations were performed at 30 °C because of excessive evaporative losses from the reaction cell at higher temperature during the course of the experiment.) The FOEB sensitivity was higher for paraoxon than parathion, which is in agreement with the model-predicted (*23*) trend based on increasing K_M values for these compounds (*20*).

The FOEB was also used to measure coumaphos, a widely used organophosphate-based insecticide. The λ_{max} (maximum absorbance wavelength) for the hydrolysis product of coumaphos, chlorferon, is 348 nm (*20*), which is far from 403 nm for *p*-nitrophenol. The important analytical characteristics of FOEB for coumaphos are given in Table 1. The data show that the sensitivity of FOEB for coumaphos was lower than that of paraoxon. This is in accordance with the model predictions based on the K_M and V_{max}/K_M values for these two compounds; a similar lower sensitivity for other OP compounds in comparison to that for paraoxon, which is the most preferred substrate, is expected. (*20*). Additionally, the extinction coefficient of chlorferon is about 2-fold lower than that of *p*-nitrophenol (*20*), which would also affect the FOEB sensitivity for coumaphos. The ability to measure the two organophosphates using different wavelength light demonstrates the potential of monitoring multiple organophosphates in mixtures. This can be achieved by scanning the light spectrum using scanning monochromators. This is an advantage of the present FOEB over the OPH-based potentiometric microbial (*17*−*19*) and enzyme (*9*) biosensors. Soman, sarin, and VX, which do not produce chromophoric products, can be monitored by measuring the fluorescence of fluoride ions released during OPH-catalyzed hydrolysis.

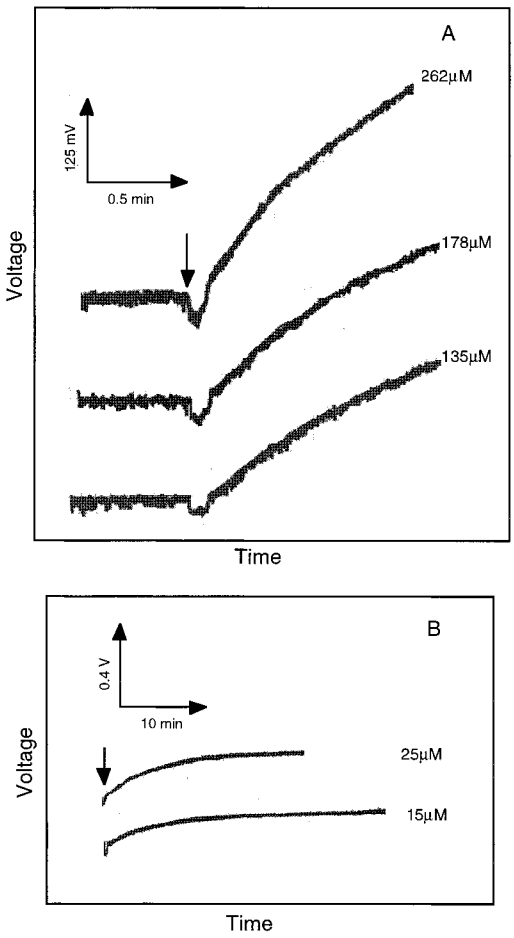

Figure 4. Representative photomultiplier tube output vs time plots for the FOEB response to paraoxon in kinetic (A) and steady-state (B) response modes. Operating conditions: 50 mM HEPES + 0.05 mM $CoCl_2$ buffer at 30 °C; 123 IU of OPH immobilized on 0.45-μm nylon membrane. Arrows show the addition of paraoxon.

Table 1. Analytical Characteristics of OPH-Modified FOEB

	steady-state response		kinetic response		
compound	sensitivity, μM^{-1}	linear range, mM	sensitivity, $min^{-1}\,\mu M^{-1}$	linear range, mM	detection limit, μM
paraoxon	0.0022	0.01−0.48	0.00092	0.02−0.5	2
parathion	0.002	0.01−0.2	nd[a]	nd	2
coumaphos	nd	nd	0.0005	5−35	5

[a] nd = not determined.

The 2 μM lower detection limit (3 times the standard deviation of the response obtained for a blank) of the FOEB based on the hydrolysis of organophosphates by the enzyme OPH and subsequent detection of the chromophoric product (developed in this research) is comparable to those of the OPH-based microbial (*17*−*19*) and enzyme (*9*) biosensors. However, this limit is still 10-fold higher than the FOEBs based on AChE inhibition (*24*,

25). This will therefore limit the applicability of the present sensor for environmental monitoring to off-line analysis. For any such application of the present FOEB, off-line sample preparation involving solvent extraction and concentration will be necessary. The present FOEB, however, will be ideal for (1) on-line monitoring of detoxification processes for treatment of wastewater generated during production and consumption of the organophosphate-based pesticides/neurotoxins, (2) selectively monitoring only the organophosphate-based pesticides/neurotoxins, and (3) monitoring individual organophosphates simultaneously in a mixture.

Model predictions for enzyme biosensors with nonreactive photometric transducers predict that enzyme biosensor sensitivity and lower detection limit can be improved by either lowering the enzyme K_M or increasing the bimolecular rate constant (*23*). Thus, it is foreseeable that a higher sensitivity and lower detection limit OPH-based FOEB will be realizable if a lower K_M and/or high bimolecular rate constant OPH is available. The advancements in enzyme engineering have made these goals potentially achievable. One such example of site-directed mutagenesis of OPH to improve the rate of hydrolysis of the chemical warfare agent soman was recently reported (*26*).

Reproducibility, Response Time, Selectivity, and Stability. The low residual standard deviation of 3.89% ($n = 6$) in the response of the FOEB for six repeated analysis of 0.09 mM paraoxon demonstrates a high precision of the new analytical tool. Similarly, a 7.7% ($n = 3$) relative standard deviation in the response of three different FOEBs to 0.42 mM paraoxon demonstrates a good reproducibility from FOEB to FOEB.

The steady-state response time (time to achieve 90% of the maximum response) for each sample depended on the analyte concentration in the test solution. The higher the concentration, the shorter the response time. For example, the steady-state response times for 9 and 135 μM paraoxon were 35 and 14 min, respectively. On the other hand, time required to analyze each sample in kinetic response mode was only 2 min. The short analysis time (2 min in kinetic mode) is far superior than the approximately 30−60 min required for analysis of each sample by the AChE-based fiber-optic biosensors (*24*−*25*) and approximately 30 min for the OPH-based flow-through microbial biosensor (*17*).

The FOEB was extremely selective for organophosphates. Other pesticides such as atrazine, sevin, sutan, pentachlorophenol, and simazine at 20 μM concentrations did not interfere. This high selectivity against other pesticides is a great advantage over the AChE-based FOEB that are interfered with by not only these pesticides but also other potential inhibitors of the AChE activity such as heavy metals (*24*, *25*). Metal chelators such as *o*-phenanthroline, ethylenediaminetetraacetate (EDTA), 2,6-pyridinedicarboxylate, cysteine, and histidine can inactivate OPH by chelating the metal ion responsible for OPH activity (*20*). However, since the concentrations at which the metal chelators inactivate OPH are very high and the rate of inactivation is very slow (*20*), no potential interference is anticipated. Dithioerythritol (DTE), dithiothreitol (DTT), and β-mercaptoethanol, which coordinate with the zinc in the OPH active site, are competitive inhibitors versus paraoxon (*20*). The presence of these compounds in an analyte sample can cause potential interference. Additionally, interference from aromatic compounds that absorb light in the UV region, in the analysis of OP compounds whose hydrolysis products have λ_{max} in the UV region, can be expected.

Table 2. Stability of the OPH-Modified FOEB

time, days	response, $(-1/I_0)dI/dt$, min^{-1}	time, days	response, $(-1/I_0)dI/dt$, min^{-1}
1	0.13	6	0.12
2	0.14	7	0.12
3	0.13	8	0.13
4	0.12	9	0.14
5	0.12	10	0.13

While the interference due to these compounds is not a problem in the kinetic response mode, in the steady-state response mode, interference from these compounds can be accounted easily for by measuring (and subtracting) the response of an "OPH-free" fiber-optic tip.

The long-term storage lifetime stability of the FOEB sensor tip was investigated by evaluating the response of the sensor to paraoxon and storing the tip at 4 °C in pH 9, 50 mM HEPES + 0.05 mM $CoCl_2$ buffer. As shown in Table 2, the biosensor was very stable over the 10-day period of investigation. On the basis of available data on the stability of free and immobilized (by cross-linking, adsorption, and covalent attachment) OPH (*2*, *9*), a stable response for at least 1 month can be anticipated. The long-term stability of the present FOEB is significantly better than that for AChE-based FOEB (*24*, *25*) because, unlike the AChE, OPH is not inactivated every time there is a reaction with organophosphates (*10*−*12*).

Conclusions

In conclusion, an OPH-modified fiber-optic enzyme biosensor for direct, rapid, and selective measurement of organophosphate nerve agents was developed. The sensor had excellent stability and selectivity. When equipped with a wavelength scanning device, the FOEB can potentially be applied for measurement of different organophosphorus esters in a mixture. In conjunction with flow injection analysis, the present FOEB will be an ideal analytical tool for long-term on-line monitoring of chemical or biological detoxification process. Additionally, the FOEB can potentially be used as a detector downstream of any chromatographic separation to determine concentrations of individual organophosphate nerve agents, for example paraoxon, parathion, and methyl parathion, where the hydrolysis product, *p*-nitrophenol, is the same or the case where the hydrolysis products have overlapping maximum absorbance wavelength.

Acknowledgment

This work was supported by grants from the U.S. EPA (R8236663-01-0) and NSF (BES9731513).

References and Notes

(1) Munnecke, D. M. Enzymatic detoxification of waste organophosphate pesticides. *J. Agric. Food Chem.* **1980**, *28*, 105−111.

(2) Caldwell, S. R.; Raushel, F. M. Detoxification of organophosphate pesticides using an immobilized phosphotriesterase from *Pseudomonas diminuta*. *Biotechnol. Bioeng.* **1991**, *37*, 103−109.

(3) Coppella, S. J.; DelaCruz, N.; Payne, G. F.; Pogell, B. M.; Speedie, M. K.; Karns, J. S.; Sybert, E. M.; Connor, M. A. Genetic engineering approach to toxic waste management: Case study for organophosphate waste treatment. *Biotechnol. Prog.* **1990**, *6*, 76−81.

(4) Mulbury, W. M.; Del Valle, P. L.; Karns, J. S. Biodegradation of organophosphate insecticide coumaphos in highly contaminated soils and liquid wastes. *Pestic. Sci.* **1996**, *48*, 149−155.

(5) Grice, K. J.; Payne, G. F.; Karns, J. S. Enzymatic approach to waste minimization in a cattle dipping operation: Economic analysis. *J. Agric. Food Chem.* **1996**, *44*, 351−357.
(6) LeJeune, K. E.; Mesiano, A. J.; Bower, S. B.; Grimsley, J. K.; Wild, J. R.; Russell, A. J. Dramatically stabilized phosphotriesterase-polymer for nerve agent degradation. *Biotechnol. Bioeng.* **1997**, *54*, 105−114.
(7) Rastogi, V. K.; DeFrank, J. J.; Cheng, T. C.; Wild, J. R. Enzymatic hydrolysis of Russian-VX by organophosphorus hydrolase. *Biochem. Biophys. Res. Commun.* **1997**, *241*, 294−296.
(8) Kolakowski, J. E.; DeFrank, J. J.; Harvey, S. P.; Szafraniec, L. L. Enzymatic hydrolysis of the chemical warfare agent VX and its neurotoxic analogues by organophosphorus hydrolase. *Biocat. Biotransform.* **1997**, *15*, 297−312.
(9) Mulchandani, P.; Mulchandani, A.; Kaneva, I.; and Chen, W. Biosensor for direct measurement of organophosphate nerve agents. 1. Potentiometric enzyme electrode. *Biosens. Bioelectron.* **1998,** in press.
(10) Marty, J.-L.; Sode, K.; Karube, I. Biosensor for detection of organophosphate and carbamate insecticides. *Electroanalysis* **1992**, *4*, 249−252.
(11) La Rosa, C.; Pariente, F.; Hernandez, L.; Lorenzo, E. Determination of organophosphorus and carbamic pesticides with an acetylcholinesterase amperometric biosensor using 4-aminophenyl acetate as substrate. *Anal. Chim. Acta* **1994**, *295*, 273−282.
(12) Dzyadevich, S. V.; Soldatkin, A. P.; Shul'ga, A. A.; Strikha, V. I.; El'skaya, A. V. Conductometric biosensor for determination of organophosphorus pesticides. *J. Anal. Chem.* **1994**, *49*, 874−878.
(13) Donarski, W. J.; Dumas, D. P.; Heitmeyer, D. P.; Lewis, V. E.; Raushel, F. M. Structure−activity relationships in the hydrolysis of substrates by the phosphotriesterase from *Pseudomonas diminuta. Biochemistry* **1989**, *28*, 4650−4655.
(14) Dumas, D. P.; Wild, J. R.; Raushel, F. M. Diisopropylfluorophosphate hydrolysis by a phosphotriesterase from *Pseudomonas diminuta. Biotechnol. Appl. Biochem.* **1989**, *11*, 235−243.
(15) Lewis, V. E.; Donarski, W. J.; Wild, J. R.; Raushel, F. M. Mechanism and steriochemical course at phosphorus of the reaction catalyzed by a bacterial phosphotriesterase. *Biochemistry* **1988**, *27*, 1591−1597.
(16) Lai, K.; Dave, K. I.; Wild, J. R. Bimetallic binding motifs in organophosphorus hydrolase are important for catalysis and structural organization. *J. Biol. Chem.* **1994**, *269*, 16579−16584.
(17) Rainina, E.; Efremenco, E.; Varfolomeyev, S.; Simonian, A. L.; Wild, J. The development of a new biosensor based on recombinant *E. coli* for the direct detection of organophosphorus neurotoxins. *Biosens. Bioelectron.* **1996**, *11*, 991−1000.
(18) Mulchandani, A.; Chauhan, S.; Mulchandani, P.; Kaneva, I.; Chen, W. A potentiometric microbial biosensor for direct measurement of organophosphate nerve agents. *Electroanalysis* **1998**, *10*, 733−737.
(19) Mulchandani, A.; Mulchandani, P.; Kaneva, I.; Chen, W. Biosensor for direct measurement of organophosphate nerve agents using recombinant *Escherichia coli* with surface-expressed organophosphorus hydrolase. 1. Potentiometric microbial electrode. *Anal. Chem.* **1998**, *70*, 4140−4145.
(20) Dumas, D. P.; Caldwell, S. R.; Wild, J. R.; Raushel, F. M. Purification and properties of the phosphotriesterase from *Pseudomonas diminuta. J. Biol. Chem.* **1989**, *33*, 19659−19665.
(21) Carr, P. W.; Bowers, L. D. Theory and applications of enzyme electrodes. In *Immobilized enzymes in analytical and clinical chemistry: Fundamentals and applications*; John Wiley & Sons: New York, 1980; pp 197−310.
(22) Rowland, S. S.; Speedie, M. K.; Pogell, B. M. Purification and characterization of a secreted recombinant phosphotriesterase (parathion hydrolase) from *Streptomyces lividans. Appl. Environ. Microbiol.* **1991**, *57*, 440−444.
(23) Schultz, J. S. Biological and chemical components for sesnors. In *Handbook of chemical and biological sensors*; Taylor, R. F., Schultz, J. S., Eds.; Institute of Physics Publishing: Bristol, U.K., 1996; pp 171−201.
(24) Andres, R. T.; Narayanaswamy, R. Fiber-optic pesticide biosesnor based on covalently immobilized acetylcholinesterase and thymol blue. *Talanta* **1997**, *44*, 1335−1352.
(25) Trettnak, W.; Reininger, F.; Zinterl, E.; Wolfbeis, O. S. Fiber-optic remote detection of pesticides and related inhibitors of the enzyme acetylcholinesterase. *Sens. Actuators B* **1993**, *11*, 87−93.
(26) Lai, K.; Grimsley, J. K.; Kuhlmann, B. D.; Scapozza, L.; Harvey, S. P.; DeFrank, J. J.; Kolakowski, J. E.; Wild, J. R. Rational enzyme design: computer modeling and site-directed mutagenesis for the modification of catalytic specificity in organophoshorus hydrolase. *Chimiai* **1996**, *50*, 430−431.

Accepted December 4, 1998.

BP980111Q